Curvature, Entropy, Congestion Management and the Power Grid

Edmond Jonckheere, Eugenio Grippo and Reza Banirazi

***Abstract*— This work develops a congestion management method for the power grid utilizing the notion of curvature. It initially uses the curvature concept to detect areas prompt to congestion (negative curvature areas) and it subsequently applies load balancing techniques (through FACTS devices) and load (storage devices) deployment to maximize curvature (grid decongestion) and cost-effectively minimize the generated energy throughout the grid, while at the same time guaranteeing stability under phase angle and voltage constraints. Two different curvature definitions are compared (Ollivier-Ricci Curvature and Effective Resistance Curvature), and an entropy concept suitable to power grid is introduced as a new measure to analyze grid congestion.**

I. Introduction

Congestion Management of the Power Grid has been extensively researched within the last few years; a comprehensive literature review can be found in [9], [10], [11], [12], [13], [14] and [15]. Within all the algorithms and strategies developed throughout the years we would mention the followings: Generator Rescheduling (GR), load shedding, Distributed Generation (DG), Optimal Power Flow (OPF), Flexible Alternating Current Transmission System (FACTS) devices, implementable via Artificial Bee Colony algorithm (ABC), Genetic Algorithms (GA) and Strength Pareto Evolutionary Algorithm (SPEA), just to name a few.

This work introduces a novel congestion management (CM) technique that basically grounds its roots in the notion of curvature. The curvature is essentially utilized to detect areas prompt to congestion (negative curvature areas); once these areas are identified via the *curvature analysis*, FACTS devices are deployed to maximize the curvature, but more practically storage devices are deployed to buses/links to reduce the flow of active power. Both deployments are dictated by the curvature analysis. To cost-effectively reduce the generation of energy throughout the entire grid, an Optimal Power Flow (OPF) algorithm is implemented to minimize the cost of energy production while maintaining stability under the usual phase angle and voltage constraints. Therefore, two objectives are simultaneously reached: grid decongestion and energy generation cost reduction.

Two curvature notions are compared: the *local* Ollivier-Ricci Curvature (definition in Sec. III) and the *global* Effective Resistance Curvature([19]). Both of them are effectively used to detect all the *critical (negatively curved) edges* prompt to transmit most of the active power within the grid. The Ollivier-Ricci Curvature (ORC) concept traces its origins back to the *earth mover's distance* idea developed in the Napoleonic era with the objective of effectively move earth from one point to the other to level off the landscape. The Earth Mover's effort is mathematically quantified as the Wasserstein 1-metric distance, and it is also known as the *transportation cost* (Gaspard Monge, 1781).

Finally, towards the end of this work, a Markov chain entropy is introduced, compared with the curvature, and applied to the power grid aiming at providing additional global information on the behavior of the grid.

A. *Outline of paper*

We begin in Section II with an overview of various simplifications of the power flow equations, the "DC power flow equations," and derive the P and Q graphs, all of which are resistive network models of the various power flows. The construction of such mathematical models will be our very first step to start analyzing the power grid. Let us emphasize that this work will analyze the IEEE 300 bus system, a benchmark example that starts by showing how an existing connection architecture with no more than 300 nodes already has congestion implications.

Sec. III summarizes the relevant literature to review the notion of curvature (namely ORC and ERC) and the notion of congestion within grids/graphs.

Sec. IV starts the construction of the proposed method for congestion management of the IEEE 300 bus system. Initially, the curvature concept is utilized to detect negatively curved lines/edges. Once the congested regions are identified, Sec. IV-B executes a heuristic procedure to simultaneously balance the loads possibly using FACTS and more practically deploying storage devices within the grid. Both allocations methods, FACTS and storages, are guided by the curvature analysis itself. While doing the heuristic tune up/allocation mentioned above, an OPF (Optimal Power FLow) algorithm is run behind the scene to secure a cost-effective generation, minimizing a quadratic generation cost functional under AC model assumptions and under constraints on the phase angles and bus voltages to secure grid stability under such changes. We emphasize the fact that the overall congestion management approach is developed and compared under both curvature notions presented in Sec. III, aiming at developing a wider range of choices that could facilitate the extension of this approach to other fields of research.

All of the simulations and methods presented till this point can be extended to take *line rating considerations* into account; this allows the method to handle realistic line limits. Sec. VII summarizes the main definitions and ideas embraced within the procedure to account for the capacity of the lines, usually determined by the thermal rating [33]. Sec. VI proposes the Entropy as an extra measure for grid analysis, exploiting the fact that ORC and Entropy are closely related.

Finally, Sec. VIII recaps what has been proposed in this work and opens up future research lines.

II. Resistive network models of power flows

Given two buses k and m specified by their voltage magnitude and phase angle pairs (V_k, θ_k) and (V_m, θ_m), resp., connected by a transmission line with admittance $Y_{km} = G_{km} - jB_{km}$, the power flow equations are well known as

$$\begin{aligned} P_{km} &= G_{km}V_k^2 + B_{km}V_kV_m\sin(\theta_k - \theta_m) \\ &\qquad - G_{km}V_kV_m\cos(\theta_k - \theta_m), \\ Q_{km} &= B_{km}V_k^2 - B_{km}V_kV_m\cos(\theta_k - \theta_m) \\ &\qquad - G_{km}V_kV_m\sin(\theta_k - \theta_m), \end{aligned}$$

where P_{km} and Q_{km} are the active and reactive power, resp., flowing from bus k to bus m. Under the standard approximations of a nearly lossless lines ($G_{km} \approx 0$) with small phase angle differences ($\theta_k \approx \theta_m$), the power flow equations are simplified to become

$$P_{km} = B_{km}V_kV_m(\theta_k - \theta_m), \quad Q_{km} = V_kB_{km}(V_k - V_m).$$

Hence, P_{km} can be viewed as the current flowing through a resistor $\rho_{km} = 1/B_{km}V_kV_m$ driven by a voltage potential difference $\theta_k - \theta_m$. Active powers injected at some buses are then modeled as currents injected at the corresponding nodes of the resistive network. Let us call this resistive network the *P-graph.*

Similarly, but subject to a discrepancy to be explained soon, Q_{km} can be viewed as the current flowing through a resistor $\rho_{km} = 1/B_{km}V_k$ driven by a voltage potential difference $V_k - V_m$. The discrepancy relative to the active power case is that the resistor is directional, $\rho_{km} \neq \rho_{mk}$. We refer to this directed resistive network as the *Q-digraph.* Ricci curvature concepts for such digraphs are developed in the context of Finsler geometry [1].

III. Curvature and Congestion

This work suggests that one of the main steps towards a succesfull congestion management method is to be able to effectively detect congestion areas. Having that in mind, this work proposes a geometric approach to the congestion management problem. Basically, we propose, as core strategy of the method, the utilization of the curvature notion to detect areas prompt to congestion (*negative curvature areas*). The bridge between negative curvature and congestion in power networks was established in [17] and [19].

As mentioned above, this work will present results utilizing *two different* curvature definitions, namely: Ollivier-Ricci Curvature and Effective Resistance Curvature.

A. Local Curvature Notion: The Ollivier-Ricci Curvature

The Ollivier-Ricci concept has recently been applied to many different fields outside mathematics itself. A clear example is the usage of ORC to differentiate biological networks corresponding to cancer cells from normal cells [7], and the detection of changes in brain structural connectivity in people with ASD (Autism Spectrum Disorders) [8]. It need not be said that ORC has been long applied in image processing too ([16]); thus, ORC as a first step in CM seems natural. The following subsection briefly defines the ORC for graphs. A better detailed review of the ORC notion can be found in [2], [3], [4], [5] and [6].

1) Wasserstein Distance, Earth Mover's Distance (EMD) and ORC: Let H be a discrete metric space equipped with a metric $d(.,.)$, and let c_{ij} be the cost of moving a unit mass from x_i to x_j; both x_i and x_j belong to H. Denote with p and q two probability distributions in H. Let $\pi_{ij} \geq 0$ be the amount of mass to be transferred from x_i to x_j. The so-called OPT (Optimal Mass Transportation) is the problem of finding an optimal transfer of mass from p to q with minimum cost. This can be formulated as ([8]):

$$\min_{\pi} \sum_{i,j} c_{i,j}\pi_{i,j}, \tag{1}$$

subject to

$$\begin{aligned} &\sum_j \pi_{i,j} = p_i, \qquad \forall i, \\ &\sum_i \pi_{i,j} = q_j, \qquad \forall j, \\ &\pi_{i,i} \geq 0, \qquad \forall i,j, \end{aligned} \tag{2}$$

where i and j are connected via an edge. If the previously formulated problem is solved with a cost $c_{i,j} = d(x_i, x_j)^r$ for any positive integer r, then it is said that the solution of the optimization problem is the r-$Wasserstein\ Distance$. Moreover, if $r = 1$, the solution is called *Earth Mover's Distance*.

Let now (X, d) be a geodesic metric space equipped with probability measures $\{p_x : x \in X\}$. Then the Ollivier-Ricci curvature $k(x, y)$ along the geodesic joining x to y is defined as

$$W_1 = (1 - k(x, y))d(x, y), \tag{3}$$

where W_1 is the EMD distance and d the geodesic distance within the space.

Recall now from Sec. II that our method will initially calculate a resistive network model called P-graph; thus, we will have a $G = (V, E, w)$ graph, where V is the set of nodes/buses, E is the set of lines/edges, and w is the set of resistances/weights. Following our previous equations, the geodesic distance $d(x, y)$ of the ORC formulation for a graph will be represented by the minimum number of steps/hops needed to go from x to y. Therefore, after this recap, a simple and short way to calculate the ORC $k(x, y)$ can be implemented through a linear programming script, and this is what has been done in the forthcoming sections.

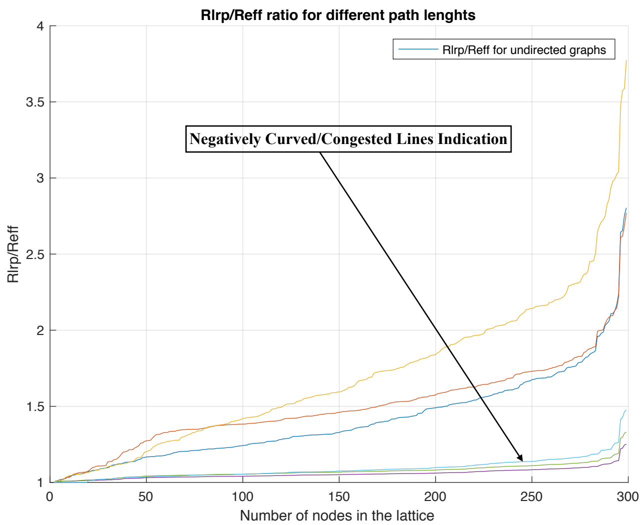

Fig. 1. Flat areas of $\rho_{\mathrm{lrp}}/\rho_{\mathrm{eff}}$ curves for the P-graph of the IEEE300 bus system indicating negative curvature along the corresponding paths

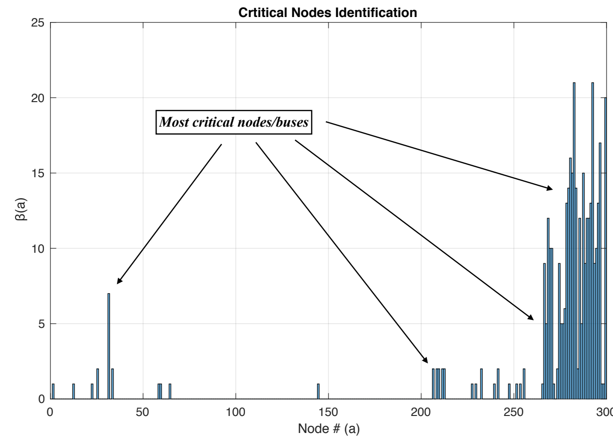

Fig. 2. Curvature centrality of critical nodes, $\beta(a)$, as per Definition 4. The height of each bar represents the number of times each critical bus appears within all critical lines.

B. Global Curvature Notion: Effective Resistance Curvature

We define the *Effective Resistance Curvature* of an idealized infinite resistive network via the fraction, already defined in [19],

$$\lim_{\rho_{\mathrm{lrp}}(k,m)\to\infty} \frac{\rho_{\mathrm{lrp}}(k,m)}{\rho_{\mathrm{eff}}(k,m)} \geq 1. \qquad (4)$$

In the above, $\rho_{\mathrm{lrp}}(k,m)$ is the resistance of the least resistive path from k to m in the network, obtained for example by the Bellman-Ford or the Dijkstra algorithm, and $\rho_{\mathrm{eff}}(k,m)$ is the effective resistance "seen" at the port km. Precisely, inject a current I at node k and draw the same current at node m; then, $\rho_{\mathrm{eff}}(k,m) := (V_k - V_m)/I$, where V_k and V_m represent voltages induced at nodes k and m, resp.

Definition 1 (Negative Effective Resistance Curvature): An infinite network is said to be negatively curved if (4) is bounded and positively curved otherwise. A finite network is said to be negatively curved if the fraction (4) is near its lower bound.

This curvature concept is specialized for power flow problems, although it has some commonalities with the Gromov [19], [20] and the Ollivier-Ricci [25] concepts. The latter is a curvature concept, *along a path* rather than at a vertex, *directly* related to transport and hence congestion.

If we construct the P-graph model (see Section II) of the IEEE300 bus network and compute the various fractions (4) for various buses, we obtain a family of curves as depicted in Fig. 1. Recall from [17], [19] that each curve corresponds to an initial node a and plots all possibles ratios $\rho_{\mathrm{lrp}}(a,k)/\rho_{\mathrm{eff}}(a,k)$ versus $k \neq a$. Given a bus a, the various k-buses are relabeled so that the various ratios $\rho_{\mathrm{lrp}}(a,k)/\rho_{\mathrm{eff}}(a,k)$ are in increasing order.

Considering $\rho_{\mathrm{lrp}}(a,k)/\rho_{\mathrm{eff}}(a,k) \geq 1$, the ratio could reach its lower bound, making the related curve "flat" with $\rho_{\mathrm{lrp}}(a,k)/\rho_{\mathrm{eff}}(a,k) \approx 1$. In this situation, most of the current (in the resistive model) or power (in the power grid) from a to k will flow along the least resistive path, hence overloading the transmission lines along that path. In the Monge-Kantorovich set up, this means that the transport is along a privileged path; in the Ollivier-Ricci curvature set up, it means that the curvature is negative.

From Fig. 1, it is clear that the IEEE300 P-graph model has several overloaded lines corresponding to flat curves. More accurate inspection reveals that there are at least 15 buses with a flattening behavior along the entire grid, which is further betrayed by the consistent congestion behavior depicted in Fig. 2 (Sec. III-C).

Conversely, if $\rho_{\mathrm{lrp}}(a,k)/\rho_{\mathrm{eff}}(a,k)$ is monotone increasing above 1, this implies that there are many paths of a resistance slightly above ρ_{lrp}, and so the current or power will be distributed along those various paths without overloading some specific ones. In the Monge-Kantorovich set up, this means that the transport is along many paths; in the Ollivier-Ricci curvature set up, it means that the curvature is positive.

Going back to Fig. 1, recall that each curve is formed by the points that represent the values of the ratio $\rho_{\mathrm{lrp}}(a,k)/\rho_{\mathrm{eff}}(a,k)$ for a fixed bus a and varying buses k.

Definition 2 (Critical Buses): A bus a is critical if its related $\rho_{\mathrm{lrp}}(a,k)/\rho_{\mathrm{eff}}(a,k)$ curve tends to be a flat line for the majority of varying buses k.

Note that various points on a $\rho_{\mathrm{lrp}}(a,k)/\rho_{\mathrm{eff}}(a,k)$ curve represent ratio values for different paths, named $(a,1),(a,2),\cdots$, and so, the curve carries information about many branches, which form different paths. Therefore, the topological information extracted from a flat curve is directly related to the transmission lines connected to its corresponding bus.

Definition 3 (Critical Lines): A critical line is a transmission line connected to a critical bus.

The critical lines/buses are responsible for most of the congestion in the grid.

*Note: this work will indistinguishably use the critical buses/lines idea for any of the two curvature notions quoted

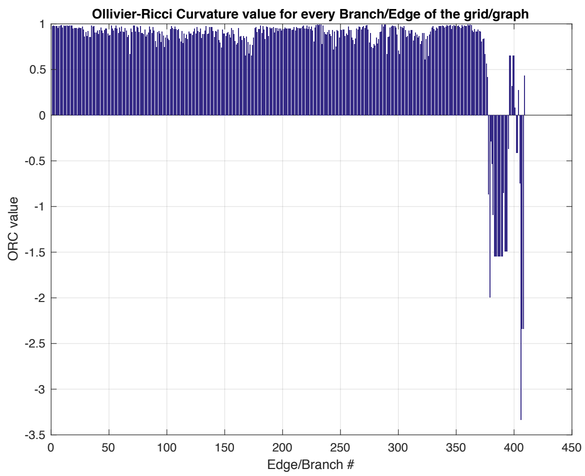

Fig. 3. Curvature Values of Critical Edges

above; thus, a critical bus/line would be the one associated with negative curvature connotation regardless of the curvature definition invoked.

C. New Curvature Centrality Concept

Different graph theoretic centrality measures specialized to the power grid can be found in the literature [18], [21]–[23]. The present work, which follows in the footsteps of [17], has the unique feature that it relates *directly* to congestion (*Def.* 2 and *Def.* 3), rather than referring to a graph-theoretic feature that can be related to congestion.

Definition 4 (Centrality): The curvature centrality $\beta(a)$ of a critical bus a is the number of times the bus a appears in the "flat" paths revealed by the $\rho_{\text{lrp}}/\rho_{\text{eff}}$ diagram.

Clearly, the flat areas of the $\rho_{\text{lrp}}/\rho_{\text{eff}}$ curves are revealing that the grid/network has serious topological defect that creates high curvature centrality (hence congestion) as evidenced by Fig. 2. Unfortunately, the topology of the grid can only be changed at significant cost, so that we will have to find less costly alternatives to manipulate the curvature.

IV. Ollivier-Ricci Curvature Driven Optimal Power Flow (ORC-OPF)

A. Negative Curvature Detection via ORC

We start this section by building up a *P-graph* of the IEEE 300 bus system; this is done following Sec. II. Once the resistive network of the power grid is acquired, we calculate the Ollivier-Ricci curvature of every edge in the model, aiming at detecting those edges that have negative curvature. Bear in mind that what we actually have is a pure resistive network model (P-graph) that can be seen as an undirected weighted graph; thus, an ORC calculation for every edge is straightforward using Sec. III.

Fig. 3 shows the ORC value for every edge in the grid. We actually have 409 edges within the grid (x-axis), and almost 25 edges show a negative ORC value (y-axis).

Observe that this brief section has identified the cause/reason to propose a congestion management procedure; it has detected the *critical edges*, which are the lines prompt to be overloaded within the grid. Therefore, if we are able to smooth over the curvature throughout the grid, we will be avoiding congestion. This is actually what is done in the next section, and it is basically a heuristic procedure that makes positively curved those areas of the grid originally negatively curved.

B. FACTS, Storage Devices and the full ORC-OPF

Recall from Sec. II that the P-graph is basically a resistive network model composed of $\rho_{km} = 1/B_{km}V_kV_m$ resistances, where k and m are the different buses of the grid ($k \neq m$), V_k and V_m are the voltages at buses k and m resp., and B_{km} is the susceptance value of the line (edge) that joins buses k and m.

Clearly, in order to change the negative curvature value of an edge, we need to change the resistance value (distance) of such edge, with the aim of obtaining a positive curvature value for it.

The only possible variables that we have available for changing the resistances are the voltages V_k and V_m, and the susceptance B_{km}, but if we leave the voltages unchanged for the grid voltage stability operations, we are only left with the susceptance value B_{km} ($\approx 1/X_{km}$).

This is actually the only choice due to the DC assumptions (mostly the $G_{km} \approx 0$ assumption), which sets the format of the ρ_{km} to be dependent only on voltages (V_k and V_m) and the susceptance (B_{km}).

This seems to be a serious limitation, because just a change in the suceptance might not be enough to do a nontrivial load balancing of the grid. Here is the approach that will be taken: for the purpose of the ORC calculation on each edge, we will enforce the DC assumptions in order to be able to have a relevant P-graph and consequently a *curvature* value for each edge. Once the curvature values are computed for all lines and the negative curvature areas are spotted, we will switch to AC conditions to smooth out the curvature (which is actually more realistic). This will allow us to have $G_{km} \neq 0$, and consequently we will have a new variable (R_{km}) to adjust, which in turn will facilitate the curvature smoothing process. Actually, while no control can be directly exercised upon the line susceptances, the apparent susceptances can be modified by, for example, FACTS series compensation to modify line impedance and static synchronous series compensator (SSSC) that connects an inductive or capacitive reactance in series with the transmission line.

This curvature smoothing process (making the negative curvature areas positive using FACTS) has been done heuristically and it was done at the same time a collection of loads were deployed in the surroundings of the critical edges. Clearly, this second stage of the proposed method allows energy storage by converting the power consumed by the deployed loads to Gibbs free energy, while at the same time minimizing the overall cost of generating active and reactive power within the grid.

Once the load balancing is performed and the loads are deployed, a new set of power flow equations are embedded in a convex optimization algorithm, with the objective of minimizing a polynomial cost function of the active and reactive power of each generator. Clearly, this is also done under the AC assumptions. We illustrate below the structure of the nonlinear programming algorithm:

Algorithm IV.1: AC COST OPTIMIZATION$(\theta, V, P_g, Q_g,)$

$\min_{\theta,V,P_g,Q_g} \sum_{k=1}^{\texttt{gensize}} \mathcal{C}_{\mathrm{AC}}(P_{g,k}, Q_{g,k}),$

subject to

$$\begin{cases} F_{\mathrm{AC}}(\theta, V, P_g, Q_g) = 0, & \\ \underline{\theta}_i \quad \leq \theta_i \leq \quad \bar{\theta}_i, & i = 1, ..., \texttt{bussize}, \\ \underline{v}_i \quad \leq v_i \leq \quad \bar{v}_i, & i = 1, ..., \texttt{bussize}, \\ \underline{P}_{\ g,k} \quad \leq P_{g,k} \leq \quad \bar{P}_{g,k}, & k = 1, ..., \texttt{gensize}, \\ \underline{Q}_{\ g,k} \quad \leq Q_{g,k} \leq \quad \bar{Q}_{g,k}, & k = 1, ..., \texttt{gensize}. \end{cases}$$

return (θ, V, P_g, Q_g)

In the algorithm, $P_{g,k}$ and $Q_{g,k}$ stand respectively for the active and reactive power generated by generator k, `gensize` is the number of generators in the grid, $x = [\theta, v, P_g, Q_g]$ is the optimization state variable where θ is the phase angle vector carrying the bus phase angle, v stands for the bus voltages vector, P_g and Q_g are respectively the vectors of active and reactive powers generated by the generators; `bussize` is the number of buses in the grid; $\mathcal{C}_{\mathrm{AC}}(.)$ is a degree-2 cost function that weights the cost of generation of each generator k:

$$\begin{aligned} \mathcal{C}_{\mathrm{AC}}(P_{g,k}, Q_{g,k}) = \alpha_{g,k}(P_{g,k})^2 + \beta_{g,k}(P_{g,k}) + \\ + \delta_{g,k}(Q_{g,k})^2 + \psi_{g,k}(Q_{g,k}) + \gamma_{g,k}. \end{aligned} \quad (5)$$

$F_{\mathrm{AC}}(\cdot) = 0$ represents the dynamic of the AC power flow. Finally, $(\underline{P}_{g,k}, \bar{P}_{g,k})$, $(\underline{Q}_{g,k}, \bar{Q}_{g,k})$, $(\underline{\theta}_i, \bar{\theta}_i)$ and $(\underline{v}_i, \bar{v}_i)$ are the min and max limits for $P_{g,k}$, $Q_{g,k}$, θ_i and v_i, respectively. Observe that the cost function is composed of $'\texttt{gensize}'$ order-two polynomials that could be built up differently for each generator; thus, we can weigh (choosing $\alpha_{g,k}$, $\beta_{g,k}$, $\delta_{g,k}$, $\psi_{g,k}$ and $\gamma_{g,k}$) each generator cost differently by shaping each polynomial separately.

The combination of the different steps made till this point constitutes what we call the Ollivier-Ricci Curvature Driven OPF (ORC-OPF), and it is summarized in Table I.

The overall procedure has been implemented in Matlab using the MATPOWER package. A modified version of the Ulas Yilmaz ORC software has been generated and implemented based on [16]. The results and a comparison with a standalone AC OPF optimization method applied to the IEEE 300 bus system are summarized in Table II. The total amount of storages deployed were 24, all of them deployed in the surroundings of critical lines. Also, a total of 30 critical lines were adjusted (load balancing) so as to maximize the curvature.

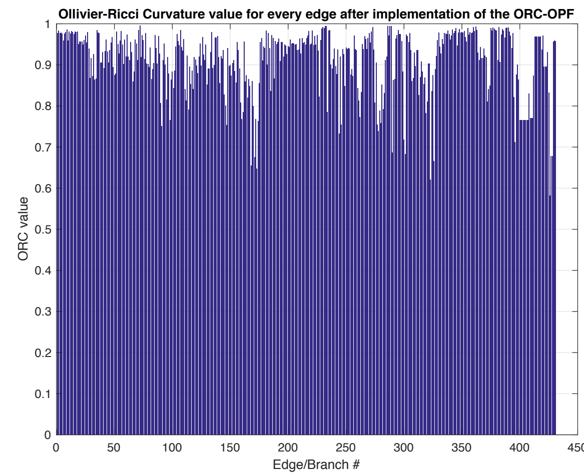

Fig. 4. Curvature Values of Critical Edges *(no negative curvature values are present)*

Observe from Table II that the optimal cost of generation proposed by the ORC-OPF spend almost 15% less energy than the optimal generation proposed by the standalone OPF; thus, these numbers clearly show the effectiveness of the proposed method. Moreover, it can be claimed now that the structure of the grid is no longer so prompt to congestion as the original one, because the ORC-OPF method not only has achieved less energy usage, but it has also smoothed over the negative curvatures areas indicated in Fig. 3. This can be clearly seen in Fig. 4, where no trace of negative ORC values can be found—and this is actually the main goal of the method. Notice that Fig. 4 shows more edges than Fig. 3; the reason is that the edges belonging to the deployed loads added after the ORC-OPF implementation have been included. We also highlight the fact that in order to calculate the ORC curvature we are using a graph abstraction, the P-graph. This is basically done because the ORC needs a graph and a distance to be computed. As a consequence, we utilize the DC assumptions to eliminate the non-linearities and generate a simple graph/model of the grid. Although we worked with AC assumptions during the load balancing and the OPF energy optimization, we analyze part of the results (curvature maximization) under the DC assumptions, because it is the fundamental tool to generate the ORC values that guide the overall method. We however choose the AC model within the main steps of the procedure, just to be closer to the real behavior of the grid, where dissipation and non-linearities are present.

V. EFFECTIVE RESISTANCE CURVATURE DRIVEN OPTIMAL POWER FLOW (ERC-OPF)

Recall that, under the *Effective Resistance Curvature* notion, the critical nodes are identified via the $\rho_{\mathrm{lrp}}(k,m)/\rho_{\mathrm{eff}}(k,m)$ tool/plots shown in Fig. 1 and such critical nodes are more clearly shown in Fig. 2 along with their centralities. This type of plots are basically showing how many transmission lines within the grid are behav-

TABLE I
OLLIVIER-RICCI CURVATURE DRIVEN OPF "MAIN STEPS"

ORC-OPF (IV-B)	identify critical buses
	adjust B's and R's (w / FACTS) of critical lines
	deploy loads around critical buses
	run AC Cost Optimization Algorithm

TABLE II
TOTAL COST FUNCTIONS VALUES (AC MODEL WITH CONVENTIONAL OPF AND WITH ORC-OPF IMPLEMENTATION)

(dollars/hr)	Total Cost Function Value
with conventional OPF	719730.00
with ORC-OPF	613730.00

ing as overloaded paths, which is captured by the ratio $\rho_{\mathrm{lrp}}(k,m)/\rho_{\mathrm{eff}}(k,m)$. In order to understand the identification of these particular paths, recall that the branches of a tree are always congested, and that their $\rho_{\mathrm{lrp}}(k,m)/\rho_{\mathrm{eff}}(k,m)$ ratios are always equal to one, because the shortest path resistance coincides with ρ_{eff} (effective resistance) in the branches of a tree. It turns out that the *Effective Resistance Curvature* notion captures more negative areas/critical buses than the ORC notion. Therefore, we should expect a better perfomance than the ORC-OPF; and this is actually the case. Applying exactly the same FACTS/storages allocation procedure done in the ORC-OPF but utilizing the critical buses depicted in Fig. 2, the overall ERC-OPF method yields the cost-reduction outcome shown in Table III. Clearly, if we compare Table II and Table III, we observe that the ERC-OPF approach utilizes an optimal set of generators that spend almost 30% less energy than the conventional OPF case, and a 20% less energy that the ORC-OPF. All these ERC-OPF improvements with respect to the ORC-OPF are easily explained by the fact that the Effective Resistance Curvature is a *global* curvature notion, and that the Ollivier-Ricci Curvature is a local edge curvature calculation; thus, the ERC captures a proper global snapshot/state of the overall grid in each step of its calculation.

The drawback of this ERC-OPC approach is that is more time consuming than the ORC-OPF due to its higher complexity. Therefore, depending on the application, an a priori suitable choice of the curvature notion before the implementation of the CM approach might be pertinent.

TABLE III
TOTAL COST FUNCTIONS VALUES (AC MODEL WITH CONVENTIONAL OPF AND WITH ERC-OPF IMPLEMENTATION)

(dollars/hr)	Cost Function Value
with conventional OPF	719730.00
with ERC-OPF	492280.00

VI. GRID ENTROPY MEASURE

This section develops an entropy-based measure suitable for weighted graphs. In our case, a weighted graph would be a P-graph resistive network model of the power grid; a graph that we have utilized to construct the two different curvature notions that gave rise to this CM approach. The idea is to define a measure that is positively correlated with the curvature increment of the grid [28]. Recall that the proposed CM method implements a curvature maximization as a core step towards an efficient cost-effective curvature driven OPF; thus, to have a topological index that measures this increment would be helpful and handy for a simple inspection of the *new curvature state* of the grid. The utilization of graph metrics to analyze the structure of networks have been extensively used in many different fields such as: computer sciences, biology and mathematical chemistry [30]. Most of this work founds its origins in the well known work of Shannon in the 1950's. Other authors further developed the entropy concept and applied it to graphs (Rashevsky, Mowshowitz, Chen *et al*, [29]). Here we'll use the R. Kazemi [30] approach:

Definition 5 (Grid Entropy): For an edge weighted graph G = (V, E, w), the entropy of G is defined by:

$$I(G,w) = -\sum_{uv\in E} p_{u,v} log(p_{u,v}) \tag{6}$$

where

$$p_{u,v} = w(u,v)/\sum_{uv\in E} w(u,v). \tag{7}$$

In our case, the weighting function *w(uv)* will be the resistance value of each *edge*. In order to be able to compare the new measure and the curvature we utilize the Global Ollivier-Ricci curvature value, which is just the average curvature value of the edge curvatures previously utilized (Fig. 3 and Fig. 4).

Although the IEEE 300 bus system presents negative curvatrue areas, the overall (average) Ollivier-Ricci curvature value is a positive quantity; thus, after the implementation of the ORC-OPF we should expect an average curvature increment within the grid. This is clearly explained by recalling that the CM approach embraces a curvature maximization. Therefore, we should also expect (as per [28]) a positive increment in the entropy; this can be observed in Table IV, where a global Ricci curvature values has been compared against the entropy of the power grid, before and after the implementations of the ORC-OPF.

TABLE IV
GLOBAL CURVATURE VALUES VS GRID ENTROPY

(IEEE300 Bus, AC P-graph)	Global ORC Value	Grid Entropy
before ORC-OPF	0.8633	5.2608
after ORC-OPF	0.9676	6.1607

As we mentioned above, the suggested CM approach maximizes the curvature; thus, it reduces the negative areas of the grid, making a more uniform or homogenous grid. Therefore, to obtain a higher entropy after the ORC-OPF implementation is natural and physically expected. If we go back to the second law of thermodynamics, we clearly have a higher entropy value (in an isolated system) as we move towards an equlibrium; and this is actually what is happening as we smooth out the curvature of the grid with the CM approach. On the other hand, an initial heterogenous state of the grid (with positive/negative curvature areas disseminated throughout the grid) cannot have another entropy value than a lower one compared with a posteriori homogenous state (after grid curvature maximization).

VII. Line Rating Considerations

As mentioned in previous sections, all of the simulations have taken into account *line rating* considerations; this has been accomplished by restricting the active power flowing through the lines to a maximum of 700MW. This is actually a way to account for the capacity of the lines, usually determined by the thermal rating [33], [35], [36].

In particular, the following definitions have been applied:

Definition 6 (DC Utilization Factor): The utilization factor for the branch (k, m) under *DC model assumptions* is defined as

$$\mu_{\mathrm{DC}} = P_{k,m}/LC_{k,m},$$

where LC stands for *line capacity*, the maximum active power allowed (in MW) through the branch (k, m).

Definition 7 (AC Utilization Factor): The *utilization factor* for the branch (k, m) under *AC model assumptions* is defined as

$$\mu_{\mathrm{AC}} = \sqrt{P_{k,m}^2 + P_{m,k}^2}/LC_{k,m}.$$

The impact of adding the line limitation constraints

$$\mu_{\mathrm{DC};\, k,m} \leq 1, \quad \mu_{\mathrm{AC};\, k,m} \leq 1,$$

in the DC and AC ORC-OPF approach is barely noticeable in the overall final cost function values for a line limit of $LC_{k.m} = 700\mathrm{MW}$, although it underlines an important advantage within the complete method: the ORC-OPF scheme is able to handle realistic line limits.

Fig. 5 shows a line utilization histogram (in percentage) for the IEEE 300 bus system with a line rating of 700 MW (on the active power of the branches) under AC analysis. As mentioned earlier, the *line rating* inclusion within the proposed load balancing encompasses a promising analysis tool: it would basically consists in the direct inclusion of *thermal rating* considerations for *bare overhead conductors*.

The increase of *thermal stress* due to variable weather or other conditions [31], [32], [35], [36] could easily trigger a line overloading that might end up in a blackout (e.g., 1996 Western North America blackout [33]). As another scenario, when a major line trips, power is rerouted along other lines

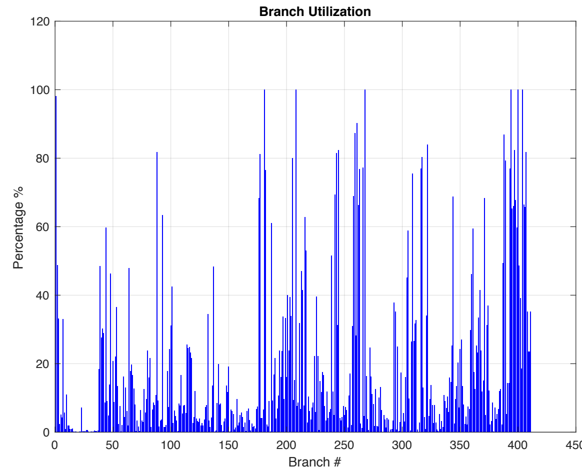

Fig. 5. *Utilization Factor* (μ_{AC}) for the AC model of the IEEE300 bus system with ORC-OPF implementations and a 700 MW active power constraint

that may not have been designed to carry such an amount of power and hence are likely to be overloaded and trip, leading to a chain reaction effect [34]. Thus, a real time power flow calculation that includes a DLR (Dynamic Line Rating [35]) could certainly help to assess power grid functionality.

VIII. Discussion and Conclusion

This work has proposed an Ollivier-Ricci / Effective Resistance Curvature based electrical load balancing procedure that can take line rating into consideration. Once the *curvature* analysis has identified the $stress\ points$, line admittances are adjusted by FACTS, loads are being deployed, and finally the generation is optimally readjusted within feasibility constraints (including line ratings) in such a way as to reduce the overall cost of generation.

It is suggested that the loads that are deployed to mitigate congestion be used to store energy, even recharge electrical vehicles, although the latter would require thorough scheduling analysis, which is left for further research.

The case-study investigated in this paper is the IEEE 300 bus system, in which load balancing immediately appears to be an issue. By choosing these nontrivial examples, the curvature analysis has revealed restrictions that the topological-combinatorial properties of the power network impose on what can be achieved in terms of load balancing. From this latter perspective, the paper has proposed to start re-thinking what can be done, and at what cost. The best option appears to be the combined load deployment/cost reduction.

As is known, the power grid is a dynamic nonlinear system acting at different time-scales, some aspects of which, like the fractal behavior of the PMU signals, are still poorly understood [26], [27]. Since it is still very unclear how the fractional dynamics betrayed by the PMU signal analysis can be used for enhanced modeling, here we have limited ourselves to utilize the AC model for combined curvature smoothing and generation cost reduction.

The new ORC-OPF / ERC-OPF optimization procedure has reduced the overall cost of generation, necessary to sustain the power flow, relative to the standalone OPF. The line rating considerations have opened a door for the future inclusion of thermal rating calculations. Towards the end of this work, a new *Grid Entropy* measure has also been presented in order to accompany the curvature analysis of the grid. This topological index basically gives a snapshot of the increment of the curvature through the maximization procedure embraced in the ORC-OPF approach, and it exploits the positive correlation between the entropy and the Ricci curvature. Finally, as a future step of this work, an optimization procedure that includes the hitherto unknown dynamical effects revealed by the data driven approach of [26], [27] could further enhance the combined curvature smoothing/cost reduction for real grids.

REFERENCES

[1] Zhongmin Shen. *Lectures on Finsler Geometry.* World Scientific, May 2001.

[2] M. DoCarmo, Riemannian Geometry., Birkhauser, Boston, 1993.

[3] Y. Ollivier A visual introduction to riemannian curvatures and some discrete generalizations In 50th Seminar of Mathematics Superior vol. 56 of CRM Proceedings and Lecture Notes, pp. 197-220, 2013.

[4] Y. Ollivier Ricci curvature of markov chains on metric spaces In Journal of Functional Analysis vol. 256, no. 3, pp. 810-864, 2009.

[5] Y. Ollivier Ricci curvature of metric spaces In Comptes Rendus Mathematique vol. 345, no. 11, pp. 643-646, 2007.

[6] S. Rachev and L. Ruschendorf Mass Transportation Problems. In vol. 1 of Probability and Its Applications, New York: Springer-Verlag, 1 ed., 1998.

[7] Romeil Sandhu, Tryphon Georgiou, Ed Reznik, Liangjia Zhu, Ivan Kolesov, Yasin Senbabaoglu and Allen Tannenbaum Graph Curvature for Differentiating Cancer Networks In Scientific reports. 5. 12323. 10.1038/srep12323, July 14, 2015.

[8] Hamza Farooq, Yongxin Chen, Tryphon T. Georgiou, Allen Tannenbaum and Christophe Lenglet Network Curvature as a Hallmark of Brain Structural Connectivity. In bioRxiv 162875; doi: https://doi.org/10.1101/162875 July 12, 2017.

[9] Nurul Idayu Yusoff, Abdullah Asuhaimi Mohd Zin, and Azhar Bin Khairuddin. Congestion Management in Power System: A Review. In *2017 3rd International Conference on Power Generation Systems and Renewable Energy Technologies (PGSRET)*, Johor Bahru, Malaysia, April 4-6 2017.

[10] A. Pillay, S. Prabhakar Karthikeyan, and D. P. Kothari. Congestion Management in Power System: A Review. In *International Journal of Electrical Power and Energy Systems*, vol. 70, pp. 83-90, 2015.

[11] K.Vijayakumar. Optimal Location of FACTS Devices for Congestion Management in Deregulated Power Systems. In *International Journal of Computer Applications*, Volume 16 No.6, February 2011.

[12] Hiren Patel and Ravikumar Paliwal Congestion Management in Deregulated Power Systems Using FACTS Devices In *International Journal of Advances in Engineering and Technology*, April 2015

[13] Vijaya Margaret and K Uma Rao. Demand Response for Residential Loads using Artificial Bee Colony Algorithm to Minimize Energy Cost. In *TENCON 2015 - 2015 IEEE Region 10 Conference*, Macao, China, Nov 1-4 2015

[14] Insoon Yang and Asuman E. Ozdaglar Reducing Electricity Price Volatility via Stochastic Storage Control. In *2016 American Control Conference (ACC)*, Boston, MA, USA, July 6-8 2016.

[15] Junjie Qin, Insoon Yang and Ram Rajagopal Submodularity of Energy Storage Placement in Power Networks. In *2016 IEEE 55th Conference on Decision and Control (CDC)*, Las Vegas, NV, USA, Dec. 12- 14 2016.

[16] Y. Rubner, C. Tomasi and L. Guibas. "The Earth Mover's Distance as a Metric for Image Retrieval". In *International Journal of Computer Vision, 40(2)*, pages pp-121, 2000.

[17] R. Banirazi and E. Jonckheere. Geometry of power flow in negatively curved power grids. In *49th IEEE Conference on Decision and Control (CDC)*, pages 6259–6264, Atlanta, GA, December 15-17 2010.

[18] Ulrik Brandes and Daniel Fleischer. Centrality measures based on current flow. In *Proc. 22nd Symp. Theoretical Aspects of Computer Sciences*, volume 3404/2005 of *Lecture Notes in Computer Science*, pages 533–544. Springer Berlin / Heidelberg, 2005.

[19] E. Grippo and E. Jonckheere. Effective resistance criterion for negative curvature: application to congestion control. In *2016 IEEE Conference on Control Applications (CCA), Part of 2016 IEEE Multi-Conference on Systems and Control*, pages 129–136, Buenos Aires, Argentina, Sept. 19-22 2016.

[20] M. Gromov. Asymptotic invariants of infinite groups. In M. A. Roller and G. Niblo, editors, *Geometric Group Theory: Proceedings of the Symposium Held in Sussex, 1991*. Cambridge University Press, 1993.

[21] Paul Hines and Seth Blumsack. A centrality measure for electrical networks. In *HICSS '08: Proceedings of the Proceedings of the 41st Annual Hawaii International Conference on System Sciences*, page 185, Washington, DC, USA, 2008. IEEE Computer Society.

[22] Zhifang Wang, Anna Scaglione and Robert J. Thomas. Electrical Centrality Measures for Electric Power Grid Vulnerability Analysis In *49th IEEE Conference on Decision and Control* , Hilton Atlanta Hotel, Atlanta, GA, USA, December 15-17, 2010.

[23] Ali Pinar, Sandip Roy and Bernie Lesieutre Power System Extreme Event Detection: The Vulnerability Frontier In *HICSS '08: Proceedings of the 41st Annual Hawaii International Conference on System Sciences* , page 184, Hawaii, HI, USA, 2008.

[24] Joaquin Mur-Amada and Jess Salln-Arasanz. Power fluctuation in a wind farm compared to single turbine. In Gesche Krause, editor, *From turbine to wind farms—Technical requirements and spin-off products*, chapter 6, pages 101–132. Intech, April 2011. ISBN 978-953-307-237-1; DOI: 10.5772/15957.

[25] Y. Ollivier. Ricci curvature on Markov chains on metric spaces. arXiv:0701886v4 [math.PR] 30 Jul 2007, 2007.

[26] L. Shalalfeh, P. Bogdan, and E. Jonckheere. Evidence of long range-dependence in power grid. In *Power and Energy Society General Meeting (PESGM)*, Boston, MA, July 2016. Available at `http://eudoxus2.usc.edu`.

[27] L. Shalalfeh, P. Bogdan, and E. Jonckheere. Kendall's tau of frequency Hurst exponent as blackout proximity margin. In *IEEE International Conference on Smart Grid Communications*, Sydney, Australia, November 06-09 2016. 978-1-5090-4075-9/16; available at `http:eudoxus2.usc.edu`.

[28] Allen Tannenbaum, Chris Sander, Liangjia Zhu, Romeil Sandhu, Ivan Kolesov, Eduard Reznik, Yasin Senbabaoglu, Tryphon Georgiou. Ricci curvature and robustness of cancer networks. http://arxiv.org/abs/1502.04512. 2015

[29] Z. Chen, M. Dehmer, Y. Shi. A note on distance based graph entropies. Entropy 16, page 54165427, 2014

[30] Ramin Kazemi. Entropy of Weighted Graphs with the Degree Based Topological Indices as Weights. *Communications in Mathematical and in Computer Chemistry,* December 2015

[31] CIGRE Working Group B2.43. Guide for Thermal Ratings Calculation of Overhead Lines. In *IEEE Transactions on Power Delivery*, December 2014

[32] IEEE Std. IEEE Standard for Calculating the Current-Temperature Relationship of Bare Overhead Conductors. page 738, 2012

[33] T. Morgan. Effect of Elevated Temperature Operation on the Tensile Strength of Overhead Conductor. In *IEEE Transactions on Power Delivery*, Vol. 11, No. 1, pages. 345-51, January 1996.

[34] Federal Energy Regulatory Commission and the North American Electric Reliability Corporation. Arizona-Southern California Outages on September 8, 2011. Causes and Recommendations. April, 2012.

[35] J. Heckenbergerova and J. Hosek, Dynamic thermal rating of power transmission lines related to wind energy integration, 11th International Conference on Environment and Electrical Engineering (EEEIC), Venice, Italy, 18-25 May 2012. (DOI: 10.1109/EEEIC.2012.6221484)

[36] H. Wan and J.D. McCalley, Increasing thermal rating by risk analysis, IEEE Transactions on Power Systems, volume 14, number 3, pp. 815 - 828, Aug. 1999.